

## Supporting Information

### **S-vacancy-mediated efficient Z-scheme photocatalytic H<sub>2</sub> generation of ultrathin nanosheet-based 2D/2D intimate heterojunction**

Li Zeng,<sup>a</sup> Li Wang,<sup>a</sup> Lei Xu,<sup>a</sup> Ping Li,<sup>a</sup> Vladimir Turkevich,<sup>c</sup> Yanyan Li,<sup>ab</sup> Jixiang Xu,<sup>\*a</sup> Lei Wang<sup>a</sup> and Haifeng Lin<sup>\*a</sup>

<sup>a</sup> *Key Laboratory of Eco-chemical Engineering, International S&T Cooperation Foundation of Eco-chemical Engineering and Green Manufacture, College of Chemistry and Molecular Engineering, Qingdao University of Science and Technology, Qingdao 266042, PR China*

<sup>b</sup> *Shandong Provincial Key Laboratory of Olefin Catalysis and Polymerization, Yellow River Delta Jingbo Chemical Research Institute Co., Ltd, PR China*

<sup>c</sup> *V. Bakul Institute for Superhard Materials, National Academy of Sciences of Ukraine, Kyiv 04074, Ukraine*

\* Corresponding author. E-mail: hflin20088@126.com, xujix47@163.com.

## Characterization results

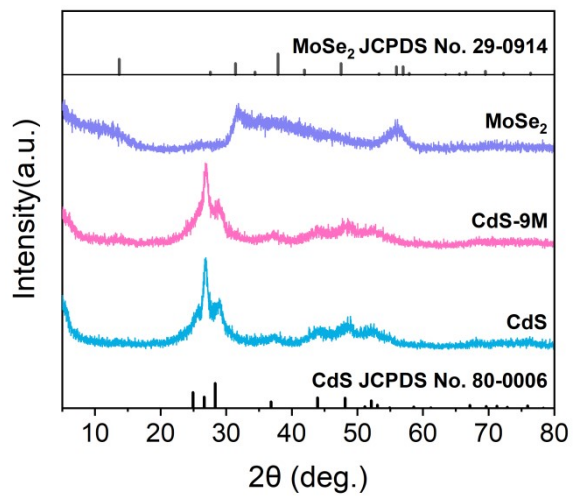


**Figure S1.** XRD patterns of MoSe<sub>2</sub>, CdS, and CdS-9M composite.

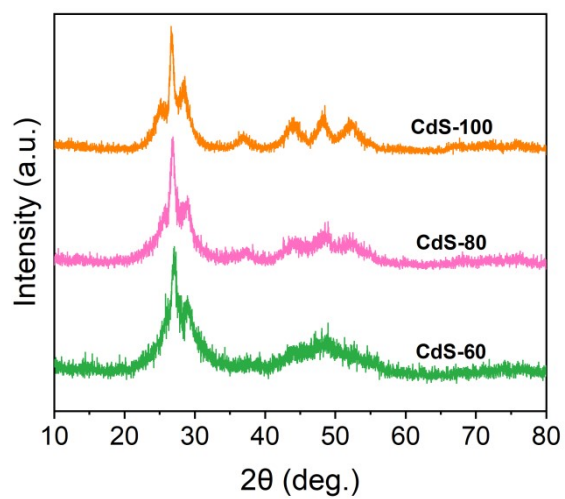


**Figure S2.** XRD patterns of CdS with varying synthesis temperatures.

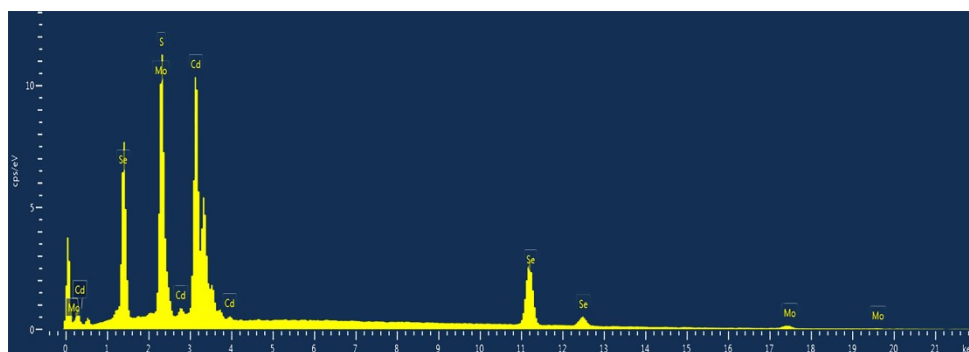


**Figure S3.** EDX spectrum of CdS-MoSe<sub>2</sub> heterojunction.

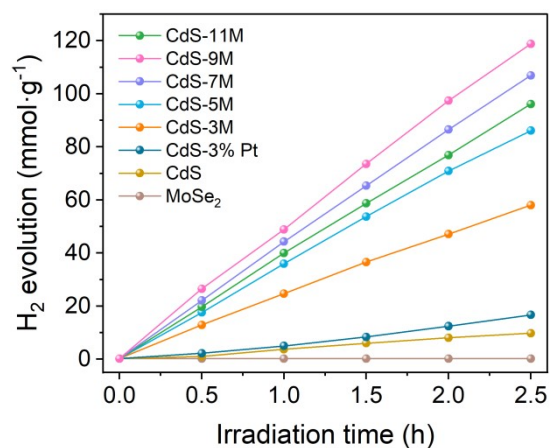


**Figure S4.** PHE activities of different samples.

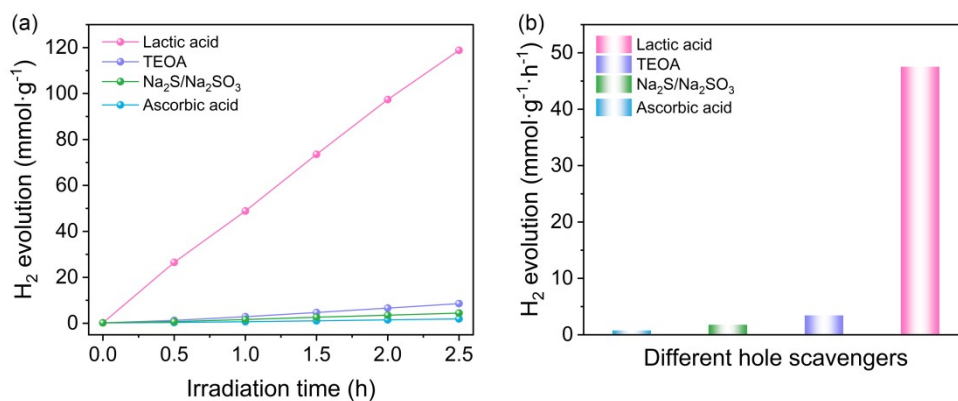


**Figure S5.** (a) PHE activities and (b) corresponding rates of CdS-9M measured with varying sacrificial agents.

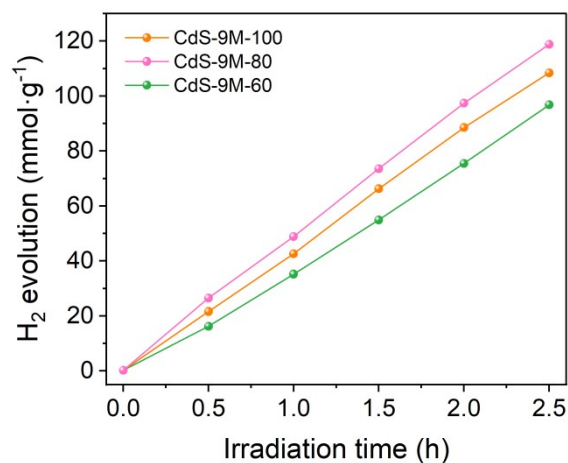


**Figure S6.** PHE activities of CdS-9M fabricated using CdS with different S<sub>V</sub> contents.

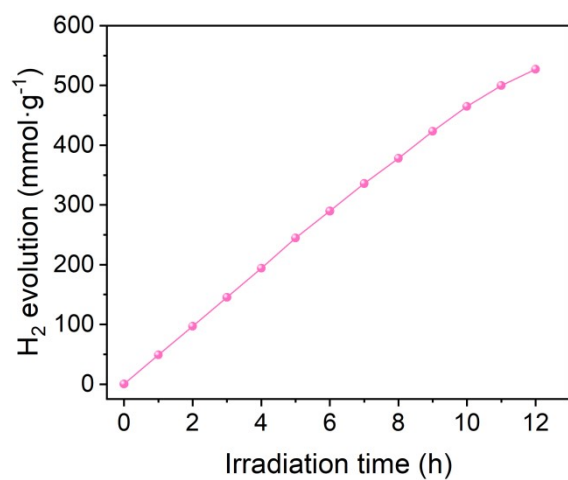


**Figure S7.** Long-term H<sub>2</sub> generation test of CdS-9M.

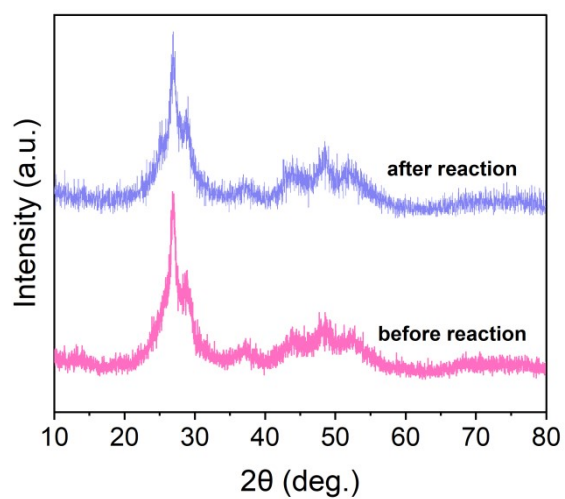


**Figure S8.** XRD patterns of CdS-9M before and after catalytic reaction.

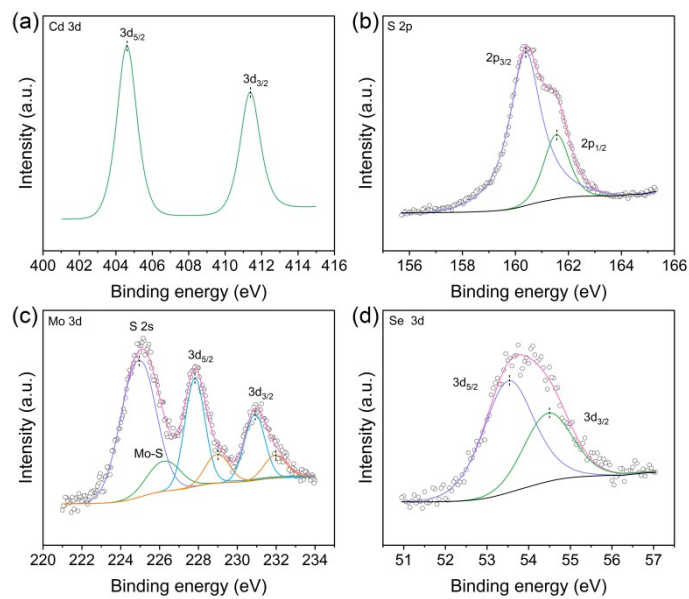


**Figure S9.** (a) Cd 3d, (b) S 2p, (c) Mo 3d, and (d) Se 3d XPS spectra of CdS-9M after H<sub>2</sub>-evolving measurement.

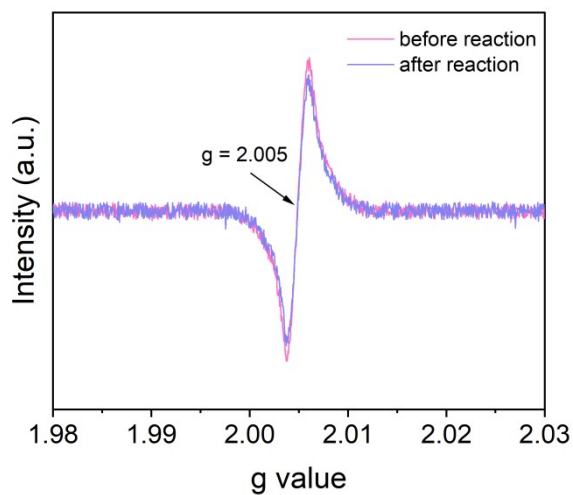


**Figure S10.** EPR spectra of CdS-9M before and after PHE test.

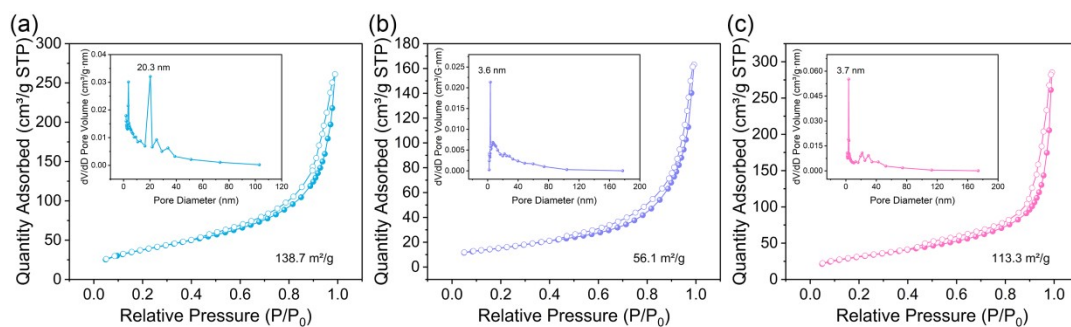


**Figure S11.** (a-c) N<sub>2</sub> adsorption-desorption isotherms and pore-size distributions (inset) of (a) CdS, (b) MoSe<sub>2</sub>, and (c) CdS-9M.

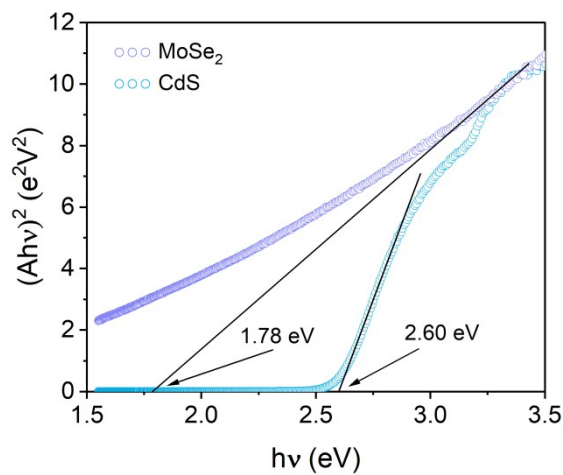


**Figure S12.** Tauc plots of CdS and MoSe<sub>2</sub>.

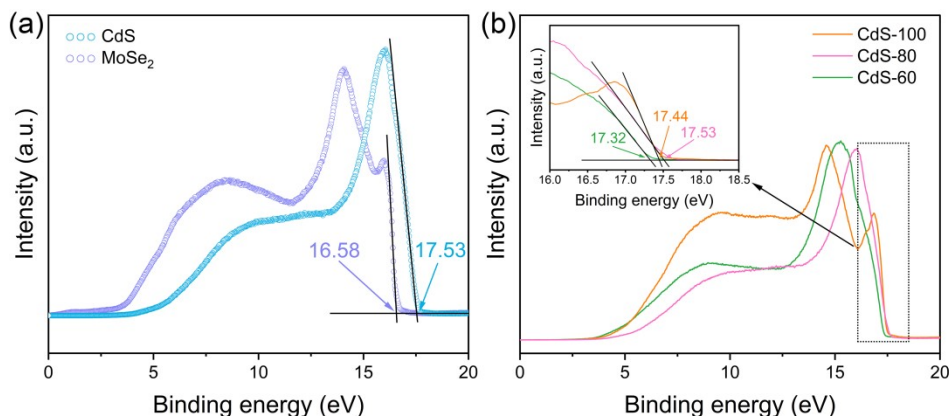


**Figure S13.** (a, b) UPS spectra of (a) CdS and MoSe<sub>2</sub> along with (b) CdS prepared with varying reaction temperatures.

The work function ( $\Phi$ ) of CdS and MoSe<sub>2</sub> was determined by the equation:  $\Phi = 21.22 \text{ eV} - E_{\text{cutoff}}$ , where 21.22 eV and  $E_{\text{cutoff}}$  represent the He(I) excitation energy and secondary cutoff binding energy, respectively.<sup>1, 2</sup> Based on the UPS spectra in Fig. S13a, the  $E_{\text{cutoff}}$  of CdS and MoSe<sub>2</sub> was recognized as 17.53 and 16.58 eV, thus their  $\Phi$  can be calculated to be 3.69 and 4.64 eV, respectively. As a result, the Fermi level ( $E_f$ ) of CdS and MoSe<sub>2</sub> was found as - 3.69 and - 4.64 eV, corresponding to - 0.81 and 0.14 V versus normal hydrogen electrode (vs. NHE), respectively.<sup>3</sup> Likewise, the  $E_f$  of CdS with differing synthesis temperatures could be discerned as - 0.60, - 0.72, and - 0.81 V vs. NHE for CdS-60, CdS-100, and CdS-80, respectively (Fig. S13b).

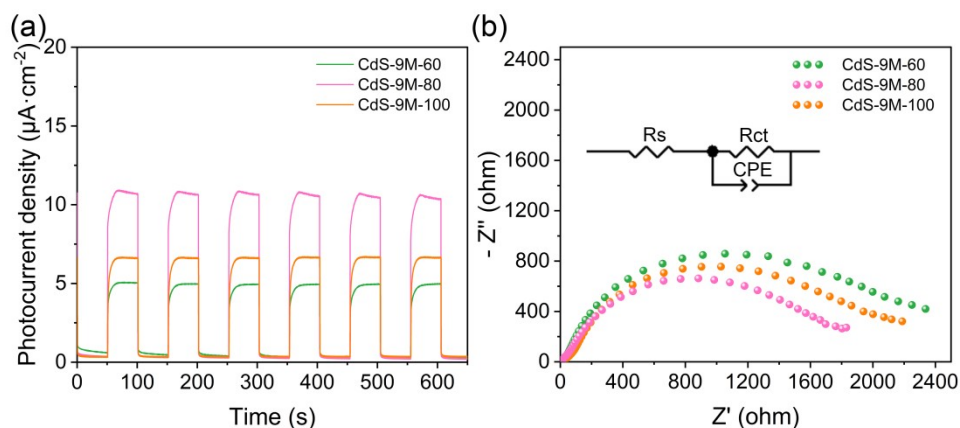


**Figure S14.** (a) Photocurrent densities and (b) EIS Nyquist curves of CdS-9M-60, CdS-9M-80, and CdS-9M-100.

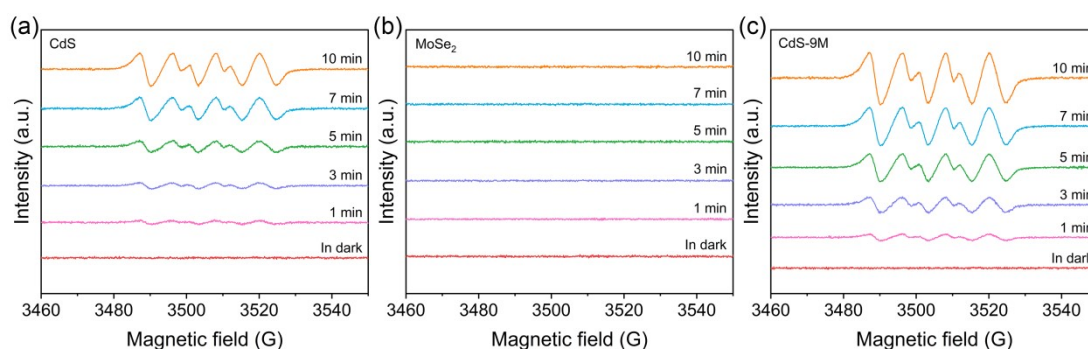


**Figure S15.** (a-c) Irradiation time-dependent EPR signals of DMPO·O<sub>2</sub><sup>-</sup> adducts produced by (a) CdS, (b) MoSe<sub>2</sub>, and (c) CdS-MoSe<sub>2</sub> composite. All figures were plotted with the identical abscissa and ordinate ranges.

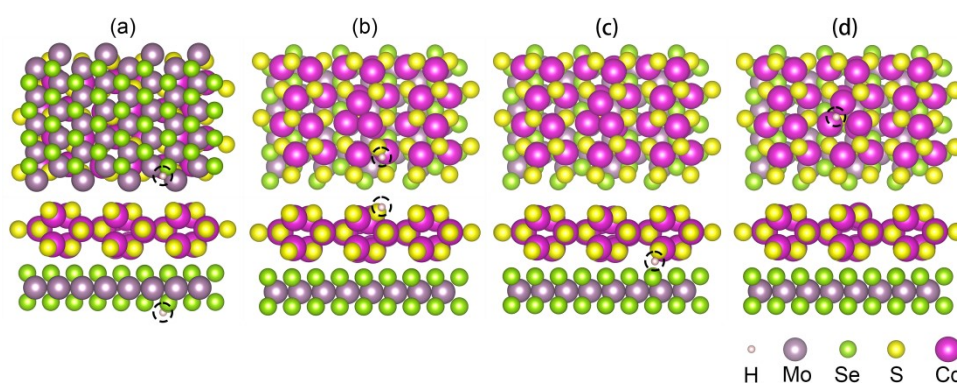


**Figure S16.** Optimized structural models of hydrogen adsorption on (a) Se site, (b) S site, (c) interface site, and (d) S<sub>V</sub> site of CdS-MoSe<sub>2</sub> heterojunction. The adsorbed hydrogen atoms were indicated by black dashed circles.

**Table S1.** Summarized PHE data of our CdS-MoSe<sub>2</sub> heterojunction and CdS-based photocatalysts reported in literatures.

Photocatalyst	Hole scavenger (aqueous solution)	Light source (Xe lamp)	Maximum rate (mmol·h <sup>-1</sup> ·g <sup>-1</sup> )	AQY (420 nm)	Reference
CdS-MoSe <sub>2</sub>	Lactic acid	λ ≥ 400 nm	47.52	18.2% 22.9% (400 nm)	This work
CdS-MoS <sub>2</sub> -CoO <sub>x</sub>	TEOA	UV-vis	7.4	7.6%	4
Cd/CdS	Na <sub>2</sub> S/Na <sub>2</sub> SO <sub>3</sub>	λ > 420 nm	10.6	12.1%	5

<b>CdS/NiCoAl-LDH</b>	Na <sub>2</sub> S/Na <sub>2</sub> SO <sub>3</sub>	$\lambda > 420$ nm	2.1	-	6
<b>CdS/WN</b>	Lactic acid	$\lambda > 420$ nm	24.13	18.59 %	7
<b>Cu-Ni/CdS</b>	Na <sub>2</sub> S/Na <sub>2</sub> SO <sub>3</sub>	$\lambda \geq 420$ nm	28.19	10.8%	8
<b>CdS@MoS<sub>2</sub>/Ti<sub>3</sub>C<sub>2</sub></b>	Lactic acid	$\lambda \geq 420$ nm	14.88	-	9
<b>Ni-CdS</b>	Na <sub>2</sub> S/Na <sub>2</sub> SO <sub>3</sub>	$\lambda > 420$ nm	20.28	13.62%	10
<b>CdS/NiS</b>	Na <sub>2</sub> S/Na <sub>2</sub> SO <sub>3</sub>	$\lambda > 420$ nm	2.18	-	11
<b>CdS/Pt/NaTaO<sub>3</sub></b>	Lactic acid	$\lambda > 420$ nm	19.8	7.9% (350 nm)	12
<b>CdS/Co<sub>3</sub>S<sub>4</sub></b>	Lactic acid	$\lambda \geq 420$ nm	23.45	18.5%	13
<b>CdS/ZnS/Bi<sub>2</sub>Se<sub>3</sub></b>	Na <sub>2</sub> S/Na <sub>2</sub> SO <sub>3</sub>	AM 1.5	7.13	8.13%	14
<b>Pt, Au/CdS</b>	TEOA	$\lambda > 380$ nm	6.71	3.72% (380 nm)	15
<b>graphdiyne/Ni-doped CdS</b>	Lactic acid	$\lambda \geq 420$ nm	13.33	4.76%	16
<b>NaZn<sub>2</sub>(OH)(MoO<sub>4</sub>)<sub>2</sub>·H<sub>2</sub>O/CdS</b>	Na <sub>2</sub> S/Na <sub>2</sub> SO <sub>3</sub>	UV-vis	17.44	9.3% (475 nm)	17
<b>CdS/Pt@NU-1000</b>	Lactic acid	$\lambda \geq 420$ nm	3.6	-	18
<b>NiS@N-doped carbon/CdS</b>	TEOA	300 nm $> \lambda >$ 1100 nm	6.1	0.66% (365 nm)	19
<b>CdS/MoB MBene</b>	Lactic acid	$\lambda \geq 420$ nm	16.89	32.9%	20
<b>ZnIn<sub>2</sub>S<sub>4</sub>/CdS</b>	Na <sub>2</sub> S/Na <sub>2</sub> SO <sub>3</sub>	$\lambda \geq 400$ nm	5.68	6.1% (400 nm)	21
<b>NiS<sub>x</sub>Se<sub>2-x</sub>/phase junction CdS</b>	Na <sub>2</sub> S/Na <sub>2</sub> SO <sub>3</sub>	$\lambda \geq 400$ nm	11.43	15.3%	22
<b>Mo<sub>2</sub>C/CdS</b>	Lactic acid	$\lambda \geq 420$ nm	19.94	13.6%	23
<b>CeO<sub>2</sub>@CdS</b>	Lactic acid	$\lambda \geq 400$ nm	8.36	56.5%	24
<b>F-TiO<sub>2</sub>/CdS</b>	Na <sub>2</sub> S/Na <sub>2</sub> SO <sub>3</sub>	UV-vis	1.70	4.3%	25
<b>CdS-CuS-NiOOH</b>	Na <sub>2</sub> S/Na <sub>2</sub> SO <sub>3</sub>	$\lambda > 420$ nm	11.36	14.4%	26
<b>Au/ZnWO<sub>4</sub>/CdS</b>	Na <sub>2</sub> S/Na <sub>2</sub> SO <sub>3</sub>	420 nm $> \lambda >$ 800 nm	5.48	2.62% (450 nm)	27
<b>CdS-MXene/MoS<sub>2</sub></b>	Lactic acid	$\lambda > 420$ nm	38.5	34.6%	28
<b>Cu<sub>2-x</sub>S/CdS</b>	Na <sub>2</sub> S/Na <sub>2</sub> SO <sub>3</sub>	$\lambda \geq 420$ nm	5.75	0.80%	29
<b>CoZnS<sub>x</sub>/CdS</b>	Lactic acid	$\lambda \geq 420$ nm	21.0	-	30
<b>Zn<sub>2</sub>MnO<sub>4</sub>/CdS</b>	Na <sub>2</sub> S/Na <sub>2</sub> SO <sub>3</sub>	UV-vis	22.42	4.15% (365 nm)	31
<b>CdNCN-CdS</b>	Na <sub>2</sub> S/Na <sub>2</sub> SO <sub>3</sub>	$\lambda \geq 420$ nm	14.7	20.50% (400 nm)	32
<b>Pd single atoms/hollow CdS</b>	Lactic acid	$\lambda > 420$ nm	22.23	14.9%	33

**Table S2.** Fitting parameters for the EIS Nyquist curves of CdS, MoSe<sub>2</sub>, and CdS-9M composites prepared using CdS with varying formation temperatures. (Rs: series resistance, Rct: charge transfer resistance, CPE: constant phase angle element)

Sample	Rs ( $\Omega$ )	Rct ( $\Omega$ )	CPE-T (F)	CPT-P
CdS	24.09	2592	$1.50 \times 10^{-4}$	0.842
MoSe <sub>2</sub>	38.06	4369	$1.89 \times 10^{-4}$	0.836
CdS-9M-60	22.11	2344	$2.20 \times 10^{-4}$	0.814
CdS-9M-80	27.41	1791	$1.65 \times 10^{-4}$	0.807
CdS-9M-100	43.35	2148	$2.07 \times 10^{-4}$	0.786

**Table S3.** XPS peak binding energies of CdS, MoSe<sub>2</sub>, and CdS-9M with and without in-situ light irradiation.

XPS species	MoSe <sub>2</sub>	CdS	CdS-9M	light-irradiated CdS-9M
Mo-S	-	-	226.2 eV	226.4 eV
Mo <sup>4+</sup>	228.3-231.4 eV	-	228.0-231.1 eV	228.1-231.2 eV
Mo <sup>5+</sup>	229.4-232.4 eV	-	228.9-231.9 eV	229.1-232.1 eV
Se <sup>2-</sup>	53.9-54.8 eV	-	53.6-54.5 eV	53.7-54.6 eV
Cd <sup>2+</sup>	-	404.3-411.0 eV	404.7-411.4 eV	404.5-411.2 eV
S <sup>2-</sup>	-	160.0-161.2 eV	160.4-161.6 eV	160.3-161.5 eV

## References

- 1 X. Wei, S. Song, W. Cai, X. Luo, L. Jiao, Q. Fang, X. Wang, N. Wu, Z. Luo, H. Wang, Z. Zhu, J. Li, L. Zheng, W. Gu, W. Song, S. Guo and C. Zhu, *Chem*, 2023, **9**, 181-197.
- 2 X. Wang, X. Wang, J. Huang, S. Li, A. Meng and Z. Li, *Nat. Commun.*, 2021, **12**, 4112.
- 3 Y. Xu and M. A. A. Schoonen, *Am. Mineral.*, 2000, **85**, 543-556.
- 4 T. Di, Q. Deng, G. Wang, S. Wang, L. Wang and Y. Ma, *J. Mater. Sci. Technol.*, 2022, **124**, 209-216.
- 5 Z. Qi, J. Chen, Q. Li, N. Wang, S. A. C. Carabineiro and K. Lv, *Small*, 2023, **19**, 2303318.
- 6 R. Yang, W. Mu, L. He, J. Meng, X. Bi, W. Luo, S. Luo and X. Lei, *Chem. Eng. J.*, 2025, **503**, 158495.
- 7 H. Liu, J. Chen, W. Guo, Q. Xu and Y. Min, *J. Colloid Interface Sci.*, 2022, **613**, 652-660.
- 8 Q. Zeng, Y. Bao, S. Ning, Q. Yu, Y. Wei and D. Zeng, *J. Mater. Chem. A*, 2024, **12**, 17286-17294.
- 9 C. Wu, W. Huang, H. Liu, K. Lv and Q. Li, *Appl. Catal. B Environ. Energy*, 2023, **330**, 122653.
- 10 F. Wu, X. Zhang, L. Wang, G. Li, J. Huang, A. Song, A. Meng and Z. Li, *Small*, 2024, **20**, 2309439.
- 11 H. Zhang, C. Shao, Z. Wang, J. Zhang and K. Dai, *J. of Mater. Sci. Technol.*, 2024, **195**, 146-154.
- 12 J. Meng, J. Zhang, Y. Huang, Z. Wang, Y. Liao, Q. Zhou, Y. Wei, L. Gao and W.-L. Dai, *Chem. Eng. J.*, 2025, **525**, 170413.

- 13 H. Huang, Y. Cai, Q. Xu, M. Xiong, L. Ding, X. Wang, Q. Jiang, Q. Li, X. Han, J. Hu and Y. Liu, *Small*, 2025, **21**, 2501710.
- 14 Y.-T. Xiong, W.-X. Liu, L. Tian, P.-L. Qin, X.-B. Chen, L. Ma, Q.-B. Liu, S.-J. Ding and Q.-Q. Wang, *Adv. Funct. Mater.*, 2024, **34**, 2407819.
- 15 Z. Fan, Q. Xu, Y. Wang, Y. Cao, X. Zeng, Y. Xie and Z. Yu, *Chem. Eng. J.*, 2025, **511**, 162016.
- 16 D. Xiang, J. Yang, H. Xie, X. Hao and Z. Jin, *Chem. Eng. J.*, 2025, **525**, 169994.
- 17 J. Liu, X. Yang, X. Guo and Z. Jin, *J. Mater. Sci. Technol.*, 2024, **196**, 112-124.
- 18 H. Yang, J. Guo, Y. Xia, J. Yan and L. Wen, *J. Mater. Sci. Technol.*, 2024, **195**, 155-164.
- 19 D. Xu, J. Ke, Z. Yan, Y. Hu and J. Liu, *Appl. Catal. B Environ. Energy*, 2025, **362**, 124746.
- 20 S. Jin, Z. Shi, R. Wang, Y. Guo, L. Wang, Q. Hu, K. Liu, N. Li and A. Zhou, *ACS Nano*, 2024, **18**, 12524-12536.
- 21 D. Zhang, Z. Gao, D. Yang, L. Wang, X. Yang, K. Tang, H. Yang, X. Zhan, Z. Wang and W. Yang, *Carbon Energy*, 2025, **7**, e707.
- 22 N. Li, Y. Qiu, L. Li, J. Zhang, Y. Gao and L. Ge, *Small*, 2025, **21**, 2408057.
- 23 J. Wu, P. Qiao, P. An, M. Zhang, H. Xiu, Z. Song, K. Li, Y. Cui, Y. Wang and W. Yao, *Appl. Catal. B Environ. Energy* 2025, **377**, 125481.
- 24 X. Chen, Q. Zhang, Y. Wang, X. Han, X. Li and P. Xu, *J. Mater. Sci. Technol.*, 2025, **238**, 86-96.
- 25 W. Fu, S. Wang, Y. Zhang, B. Cheng and Y. Wu, *J. Mater. Sci. Technol.*, 2025, **232**, 181-190.
- 26 H. Lin, M. Kong, Z. Zou, X. Li, H. Wang, J. Xu, V. Turkevich, Y. Li, X. Wang and L. Wang, *Small*, 2025, **21**, 2410751.
- 27 W. Wu, N. Zhang and Y. Wang, *Adv. Funct. Mater.*, 2024, **34**, 2316604.
- 28 K. S. Ranjith, A. Mohammadi, G. S. R. Raju, Y. S. Huh and Y.-K. Han, *Nano Convergence*, 2024, **11**, 51.
- 29 K. Bang, B. Park, J.-Y. Jung and H. Song, *Small Struct.*, 2025, **6**, 2500468.
- 30 L. Song, K. Lin, D. Feng, B. Ma and F. Zhang, *Appl. Catal. B Environ. Energy*, 2025, **379**, 125657.
- 31 F. Liu, X. Li, B. Sun, Y. He, T. Gao and G. Zhou, *J. Mater. Sci. Technol.*, 2026, **250**, 233-242.
- 32 T. Huang, Z. Huang, X. Yang, S. Yang, Q. Gao, X. Cai, Y. Liu, Y. Fang, S. Zhang and S. Zhang, *Adv. Powder Mater.*, 2024, **3**, 100242.
- 33 Z. Huang, C. Guo, Q. Zheng, X. Long, J. Fan, P. Ma, Y. Dong, A. N. Alodhayb, Z. Chen, D. Wang and X. Yi, *J. Energy Chem.*, 2025, **108**, 210-220.